

A Chiral 28-Membered Macrocycle with Symmetry and Structure Similar to That of *trans*-Cyclooctene

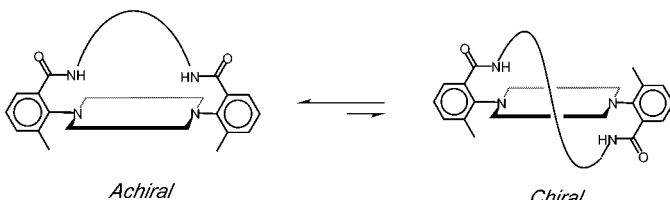
Charles F. Degenhardt III, Mark D. Smith, and Ken D. Shimizu*

Department of Chemistry and Biochemistry, University of South Carolina,
Columbia, South Carolina 29208

shimizu@mail.chem.sc.edu

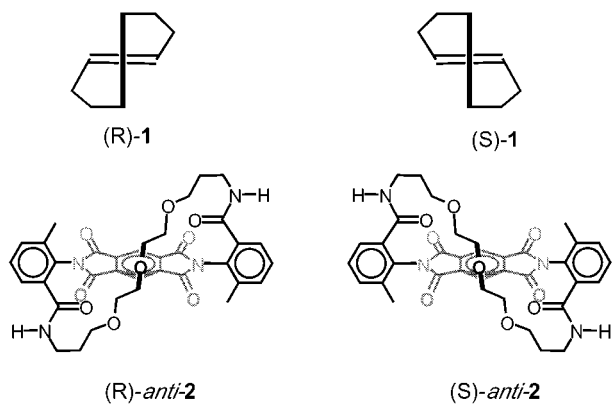
Received December 11, 2001

ABSTRACT



A bridged *N,N*-di(aryl)-1,2,4,5-benzenediimide was synthesized in which restricted rotation led to two diastereomeric conformations at room temperature. The more stable *syn*-macrocycle is achiral, whereas the strained *anti*-macrocycle possesses planar chirality similar to that of *trans*-cyclooctene. The structure was characterized by X-ray crystallography, and the enantiomers were resolved by chiral chromatography.

One of the most interesting and well-studied systems having planar chirality is *trans*-cyclooctene (**1**), in which chirality arises from conformational restriction.^{1,2} The molecule adopts stable enantiomeric conformations, (*R*)- and (*S*)-**1**, in which the hexane chain bridges either around the front or back of the double bond.



As a result, the *trans*-double bond is highly strained and undergoes reactions under unusually mild conditions, often

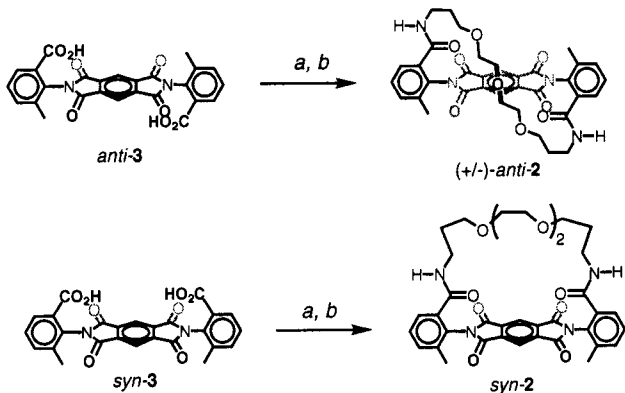
with high facial selectivity. In contrast, the corresponding *cis*-cyclooctene is considerably more stable and achiral.

We present, herein, topologically analogous 28-membered macrocycles, *syn*-**2** and *anti*-**2**, that possess planar chirality, ring strain, and conformational isomerism similar to that of *trans*- and *cis*-cyclooctene, respectively. Macrocycle **2** adopts stable diastereomeric *syn*- and *anti*-conformations (Scheme 1) in which the carboxylic amide groups can be on the same or opposite sites of the diimide surface. The stability of these conformers arises from restricted rotation about the two $\text{N}_{\text{imide}}-\text{C}_{\text{aryl}}$ single bonds of the 1,2,4,5-benzenediimide surface.³ In the *syn*-macrocycle, the triethyleneglycol linker can easily bridge the two convergent amide groups. Consequently, *syn*-**2** is the more stable isomer and is achiral. The *anti*-macrocycle, on the other hand, has some ring strain due to the necessity of the linker to wrap around the benzene-

(1) Cope, A. C.; Pawson, B. A. *J. Am. Chem. Soc.* **1965**, *87*, 3649–3651.

(2) (a) Schlägl, K. *Top. Curr. Chem.* **1984**, *125*, 27–62. (b) Nakazaki, M.; Yamamoto, K.; Naemura, K. *Top. Curr. Chem.* **1984**, *125*.

(3) (a) Curran, D. P.; Geib, S.; N, D. *Tetrahedron* **1999**, *55*, 5681–5704. (b) Verma, S. M.; Singh, N. D. *Aust. J. Chem.* **1976**, *29*, 295–300. (c) Kishikawa, K.; Yoshizaki, K.; Kohmoto, S.; Yamamoto, M.; Yamaguchi, K.; Yamada, K. *J. Chem. Soc., Perkin Trans. I* **1997**, 1233–1239.

Scheme 1^a

^a (a) Oxalyl chloride, catalytic DMF, CH_2Cl_2 ; (b) $\text{NH}_2(\text{CH}_2)_3\text{O}-(\text{CH}_2\text{CH}_2\text{O})_2(\text{CH}_2)_3\text{NH}_2$ (**4**), triethylamine, CH_2Cl_2 (25% and 35% yield for *anti*-**2** and *syn*-**2**).

diimide surface. The linker in *anti*-**2** can connect around either the front or back of the molecule, leading to enantiomeric conformations. Similar twisted atropisomeric macrocyclic systems have been reported with “strapped” tetraaryl porphyrins; however, in these systems, the enantiomeric conformations were not stable at ambient temperatures.^{4,5} The enantiomeric conformations of *anti*-**2**, in contrast, are stable at room temperature and could be resolved.

Macrocycle **2** was synthesized by bridging the carboxylic acids of the previously reported atropisomeric diacid **3** (Scheme 1).⁶ Restricted rotation in **3** was evident by the isolation and separation of two stable diastereomeric conformations, *syn*- and *anti*-**3**, having carboxylic acids fixed on the same and opposite sides. The atropisomers were sufficiently stable that macrocyclization could be carried out without isomerization. Thus, treatment of *anti*-**3** with oxalyl chloride yielded the corresponding diacid chloride that was subsequently reacted with diamine **4** to afford macrocycle (\pm) -*anti*-**2**.⁷ Likewise, the macrocyclization of *syn*-diacid **3** yielded the corresponding *syn*-**2**.

In each case, macrocyclization to form the 28-membered rings proceeded in relatively good yields (25% and 35% for *anti*- and *syn*-**2**) without having to resort to high dilution conditions (~ 20 mM). This was not surprising for *syn*-**3** in which the convergent diacids are preorganized by the rigid diimide framework. However, similar yields were also achieved for *anti*-**3** in which the carboxylic acids are on opposite faces of the molecule and modeling showed that the oligo(ethylene glycol) linker would just barely span the

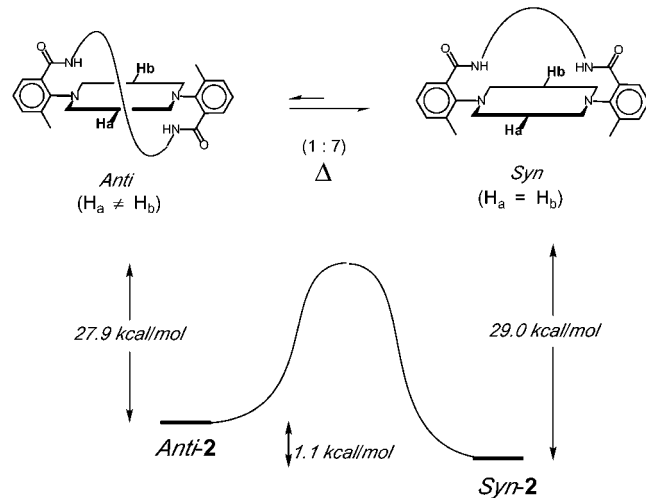
(4) Redman, J. E.; Sanders, J. K. M. *Org. Lett.* **2000**, 2, 4141–4144.
(5) Gunter, M. J.; Johnston, M. R.; Skelton, B. W.; White, A. H. *J. Chem. Soc., Perkin Trans. 1* **1994**, 1009–1018.

(6) Degenhardt, C., III; Shortell, D. B.; Adams, R. D.; Shimizu, K. D. *J. Chem. Soc., Chem. Commun.* **2000**, 929–930.

(7) ¹H NMR (400 MHz, CDCl_3) δ 8.72 (s, 1 H), 8.49 (s, 1 H), 7.49 (d, 2 H, $J = 7.5$ Hz), 7.44–7.37 (m, 4 H), 6.08 (dd, 2 H, $J = 4.0$ and 8.5 Hz), 3.87–3.40 (m, 14 H), 2.75–2.85 (m, 2 H), 1.60–1.75 (m, 4 H), 2.32 (s, 6 H). HRMS (FAB, NBA) calcd for $\text{C}_{36}\text{H}_{37}\text{N}_4\text{O}_9$ 669.2560 (M^{+}); found 669.2557. Anal. Calcd for $\text{C}_{36}\text{H}_{36}\text{N}_4\text{O}_9 \cdot \text{CH}_3\text{CO}_2\text{CH}_2\text{CH}_3$: C, 63.48; H, 5.86; N, 7.40. Found: C, 63.73; H, 5.68; N, 7.80. First eluting enantiomer $[\alpha]_D = -65.5$. Second eluting enantiomer $[\alpha]_D = +58.7$.

anti-diacids. A possible explanation for the relatively high yield of the *anti*-macrocycle may lie in the choice of the oligo(ethylene glycol) linker. This linker adopts a folded or bent conformation as opposed to an *all-anti*-linear conformation of an alkane, which has been exploited in a number of curved supramolecular systems.^{8,9}

The isomeric relationship between *syn*- and *anti*-**2** was established from heating studies. The compounds interconverted on heating, with an equilibrium ratio of 7:1 (*syn*-/*anti*-) in *i*-PrOH, which corresponds to a 1.1 kcal/mol energy difference between the two isomers with the *syn*-isomer being the more stable. The observed equilibrium ratio was consistent with molecular modeling studies (MM2) that predicted an energy difference of 0.79 kcal/mol.¹⁰ The kinetic stability of the atropisomeric macrocycles was measured by following the rate of equilibration. The barrier of *anti*-**2** to *syn*-**2** was measured in isopropyl alcohol at 82 °C. A half-life of 2.0 h was observed, corresponding to a barrier of rotation of 27.9 kcal/mol (Scheme 2). The rotational barrier of the reverse

Scheme 2. Representations and Energy Diagram of the Interconversion of *syn*- and *anti*-**2**

isomerization of *syn*-**2** to *anti*-**2** is 29.0 kcal/mol and was calculated as the sum of the *anti*-**2** to *syn*-**2** barrier (27.9 kcal/mol) and the destabilization energy of the *anti*-**2** isomer (1.1 kcal/mol). This value is consistent with that measured for the parent diacid **3**, 29.4 kcal/mol.⁶

TLC, NMR, and X-ray crystallography provided confirmation of the structures of macrocyclic *syn*- and *anti*-**2**. The isomers were easily differentiated by TLC. Similar to other atropisomeric *N,N*-diaryl diimide and phorphyrin systems, the higher dipole moment *syn*-**2** was initially assigned as the

(8) Meyer, S.; Louis, R.; Metz, B.; Agnus, Y.; Varnek, A.; Gross, M. *New J. Chem.* **2000**, 24, 371–376.

(9) Preece, J. A.; Stoddart, J. F. *Macromol. Symp.* **1995**, 98, 527–540.

(10) Molecular modeling was carried out using MacroModel 5.5 using MM2 forcefield with CHCl_3 as solvent. The *syn*- and *anti*-conformers were individually minimized using Monte Carlo conformational search with 1000 structures.

lower R_f isomer and the lower dipole moment *anti*-2 assigned as the higher R_f isomer.¹¹

This preliminary assignment was confirmed by their characteristic symmetries as measured by ^1H NMR (Figure 1). In the case of *syn*-2, the 1,2,4,5-benzenediimide surface

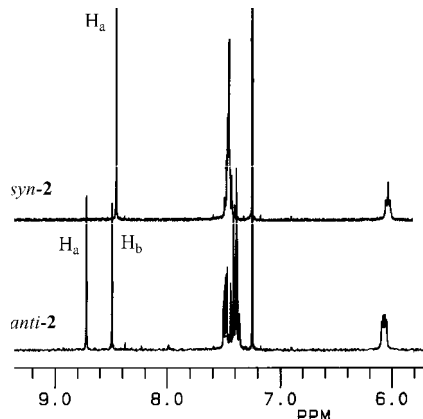


Figure 1. ^1H NMR spectra of *syn*- and *anti*-2 in CDCl_3 . Asterix denotes CHCl_3 solvent peak.

is symmetrical and the corresponding 3- and 6-aryl protons (H_a and H_b) are chemically equivalent (Scheme 2). In contrast, the 1,2,4,5-benzenediimide surface of *anti*-2 is desymmetrized by the proximity of the linker to one edge and H_a and H_b are chemically inequivalent. Accordingly, the ^1H NMR of *anti*-2 shows two singlets for protons H_a and H_b , each integrating for one proton. The lower symmetry of *anti*-2 was also evident in the triethylene glycol linker as the protons of the CH_2 group nearest the amide bond were diastereotopic with a large geminal coupling.

Conformation of the macrocyclic structure and isomer assignments was provided by an X-ray crystal structure of *anti*-2 (Figure 2).¹² Racemic *anti*-2 was recrystallized by slow evaporation from $\text{EtOAc}/\text{CH}_2\text{Cl}_2$. The twisted conformation of the *anti*-conformation was evident with the oligo(ethylene glycol) linker tucked around the diimide spacer. The imide nitrogens are bent somewhat out of planarity; however, the energetic penalty is relatively low as this structural deformation is present in other diimide structures that are not bridged or strained.¹³

Resolution of *anti*-2 was accomplished by chiral HPLC using a ChiralPak AD column (Figure 3). The enantiomers of *anti*-2 were well separated from each other as well as from the diastereomeric *syn*-2. The large separation factor

(11) (a) Shimizu, K. D.; Dewey, T. M.; Rebek, J. *J. Am. Chem. Soc.* **1994**, *116*, 5145–5149. (b) Chong, Y. S.; Smith, M. D.; Shimizu, K. D. *J. Am. Chem. Soc.* **2001**, *123*, 7463–7464. (c) Sanders, G. M.; Van Dijk, M.; Machiels, B. M.; van Veldhuizen, A. *J. Org. Chem.* **1991**, *56*, 1301–1305.

(12) Crystal data for *anti*-2: $((\text{C}_{36}\text{H}_{36}\text{N}_4\text{O}_9)_2\text{C}_6\text{H}_8)_2$. Crystal data: colorless block, $0.36 \times 0.30 \times 0.21 \text{ mm}^3$, $T = 213(2)$ K. Monoclinic, $\text{P}2_1/c$; $a = 19.922(2)$ \AA , $b = 15.346(1)$ \AA , $c = 27.780(2)$ \AA , $\beta = 91.292(2)$, $V = 8491.0(12)$, $Z = 4$. $R_1(F) = 0.067$, $\text{wR}2(F^2) = 0.153$ for 5796 reflections with $I > 2\sigma(I)$. For complete data, see Supporting Information.

(13) Shimizu, K. D.; Dewey, T. M.; Rebek, J. *J. Am. Chem. Soc.* **1994**, *116*, 5145–5149.

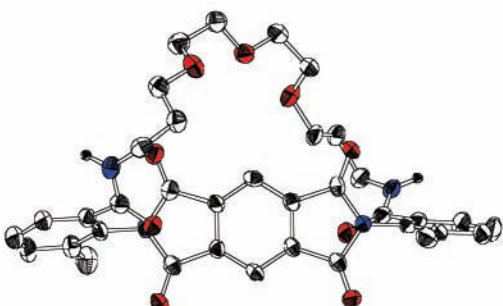
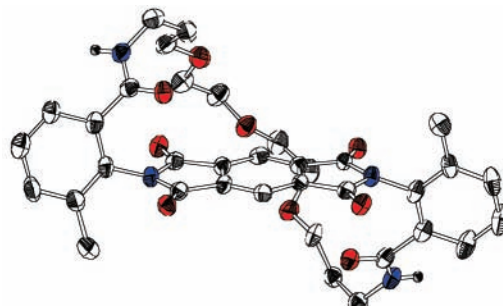


Figure 2. Top and side views of X-ray crystal structure of *anti*-2. Hydrogens have been removed for viewing clarity.

(α) of 5.0 between enantiomers enabled semipreparative resolution of *anti*-2 with an analytical column (4.5 mm \times 250 mm). The chirality and enantiomeric relationship between the first two compounds was demonstrated by their opposite optical rotation. The more quickly eluting enantiomer showed $[\alpha] = -65.5$ ($c = 0.041$, CH_2Cl_2), and the second more slowly eluting enantiomer showed a slightly smaller but opposite optical rotation, $[\alpha] = +58.7$ ($c = 0.043$, CH_2Cl_2). The lower optical purity (91.5%) of the second (+)-enantiomer was due to some of the first peak tailing into the second, which was confirmed by reinjection on the chiral HPLC. Otherwise, the compounds were identical by NMR and TLC.

The enantiomeric relationship between the two compounds was further established from their mirror image CD spectra

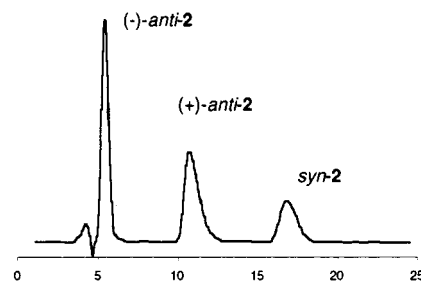


Figure 3. HPLC trace for mixture of (\pm) -*anti*-2 (first two peaks) and *syn*-2 (third peak). Conditions were ChiralPak AD, 0.8 mL min^{-1} in *i*- PrOH/Hex (60:40).

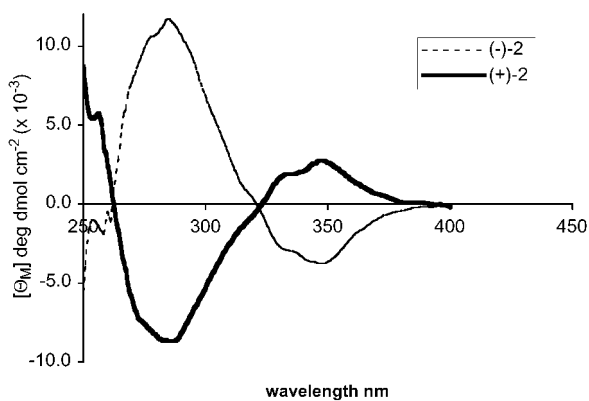
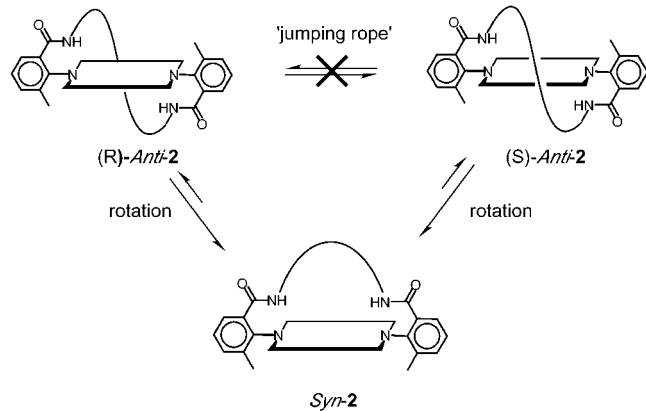


Figure 4. CD spectra of enantiomers of *anti*-2.

(Figure 4). Again, the slightly smaller Cotton effects of the (+)-enantiomer was consistent with its lower enantiomeric purity.

The enantiomers of *anti*-2 could interconvert by either of two mechanisms (Scheme 3). Racemization can occur directly by the macrocycle “jumping rope” or through the intermediacy of the *syn*-isomer by sequential rotation about

Scheme 3. Representations of Mechanisms of Enantiomer Interconversion of *anti*-2



the two $C_{\text{aryl}}-\text{N}_{\text{imide}}$ bonds. The stability of the enantiomers of *anti*-2 demonstrates that both processes are slow at room temperature; however, it does not differentiate which mechanism is operative. In the case of *trans*-cyclooctene, both mechanisms are observed, but the “jumping rope” mechanism is lower in energy.¹⁴

Thermal racemization studies of enantiomerically pure *anti*-2 demonstrated the intermediacy of *syn*-2, which is formed in higher concentrations than either *anti*-conformer (Scheme 3). Furthermore, the rate of equilibration of the enantiomers is tied to the rate of rotation about the $C_{\text{aryl}}-\text{N}_{\text{imide}}$ bonds. Thus, enantiomer interconversion likely occurs via rotation of one $\text{N}_{\text{imide}}-\text{C}_{\text{aryl}}$ bond to yield *syn*-2 followed by rotation of the second $\text{N}_{\text{imide}}-\text{C}_{\text{aryl}}$ bond to yield (ent)-*anti*-2. This pathway is consistent with molecular modeling studies that predict that the oligo(ethyleneglycol) linker is too short to allow the jumping rope mechanism.¹⁴

In conclusion, bridged aryl diimide 2 was synthesized in which restricted rotation leads to the formation of two diastereomer conformations. The two stable, separable diastereomers consisted of a lower energy *syn* conformation and a higher energy *anti* conformation. The diastereomers interconverted on heating, with an equilibrium ratio of 7:1 (*syn*/*anti*-). The *anti* conformation provided an interesting example of planar chirality resulting in two enantiomers. X-ray crystallography of the racemic mixture confirmed the structure of the chiral *anti* conformation. The enantiomers were resolved by chiral chromatography and further studied by optical rotation, CD spectroscopy, molecular modeling, and heating studies. Unlike *trans*-cyclooctene, interconversion of the two enantiomers probably occurs first primarily via bond rotation to give the more stable *syn*-diastereomer as opposed to the “jumping rope” mechanism.

Acknowledgment. We acknowledge support of this research from the NSF (DMR 9807470).

Supporting Information Available: Experimental procedures for the synthesis of *syn*- and *anti*-2 and CIF files for the X-ray structure of *anti*-2. This material is available free of charge via the Internet at <http://pubs.acs.org>.

OL0172119

(14) Molecular modeling studies were performed using MacroModel 5.5 using an MM2 forcefield.